Prototyping a new car semi-active suspension by variational feedback controller

G. Pepe[1], N.Roveri[1], A. Carcaterra[1]
[1]Dept. of Mechanical and Aerospace Engineering,
Sapienza University, Rome, Italy
e-mail: **gianluca.pepe@uniroma1.it**

Abstract
New suspension systems electronically controlled are presented and mounted on board of a real car. The system consists of variable semi-active magneto-rheological dampers that are controlled through an electronic unit that is designed on the basis of a new optimal theoretical control, named VFC-Variational Feedback Controller. The system has been mounted on board of a BMW Series 1 car, and a set of experimental tests have been conducted in real driving conditions. The VFC reveals, because of its design strategy, to be able to enhance simultaneously both the comfort performance as well as the handling capability of the car. Preliminary comparisons with several industrially control methods adopted in the automotive field, among them skyhook and groundhook, show excellent results.

1 Introduction: key-performance-indexes of suspension systems

A first application to semi - active control of VFC-Variational Feedback Control has been considered to enhance suspension performance of a motor vehicle and presented in [1-6]. There, the control logic was applied in a context of numerical simulations, optimizing comfort and handling, minimizing the car body acceleration and maximizing the road-tire contact force.

This paper proceed ahead in this direction, describing the prototyping activities to install a complete integrated device based on VFC on a real vehicle. Namely, this research is motivated by the fact that the VFC control logic is capable of reaching excellent compromise performances between handling and comfort, not usual in others control systems.

In fact, when designing a new suspension concept, many physical parameters contribute to the final performances of the system. For example, the comfort ability is frequently related to the chance of mitigating the vertical accelerations on the car seats, while the handling ability of the car is indeed related to the tire grip the suspension system can assure by preventing sudden decreasing of the load on the road. Beside this, for example, also the stroke of the suspension is an important physical response to limit. It is clear, in fact, that it is easy to reduce the car body acceleration if one can accept large deflections of the elastic elements of the suspension system. The acceleration reduction is indeed much more difficult to achieve if a severe constraint is demanded on the maximum admissible stroke. At the same time, the settling time is an important parameter in the suspension performance, but not specifically related to the comfort or handling, and it deserves its own emphasis at the suspension design stage.

In this paper, a set of key-performance-indexes are defined and systematically considered to provide a general optimal control of the suspension system. In particular these parameters, considered as pair to be associated to the x and y axes, can in turn define special performance-planes. In these planes can be identified regions of performances that can be associated to the different existing suspension control logics. In this sense, the ability of a new method of control can be measured by its capability of reaching zones that are indeed prohibited to the conventional strategies.

Probably the best way to introduce VFC and its application to car dynamics, is to present its performances emphasizing its capability to intrude into difficult areas of the performance planes, reveling the ability to combine different, and frequently antithetic, characteristics of the suspension.

The VFC is here first applied to a half-car, instead of considering the more usual quarter-car. The choice for the use this more complete model to explore the performance of the suspension system, is motivated by the fact the pitch and heave dynamics coupled together, permits to verify the controlled response in a more realistic way. In fact, the suspension is not only asked to prevent large accelerations at the point of attachment of the suspension to the body (what is done , for example, in the context of the quarter-car), but we need to verify the quality of control observing the motion of the passengers seats, that comes out as a combination of the pitch and heave motion excited by the complete suspension system of the car. Moreover, we would like to take into account different abilities of the suspension to be faced with different types of excitations: surely, random excitation coming from a rough road to be filtered is a good figure to rank the suspension job, but this attitude would be compared with the bump-response, that generally is achieved acting on a completely different type of settings.

In this view, there are many parameters to be monitored for the half car, for example displacement-stroke, acceleration of the wheel and of the car body and settling time after a bump crossing, tire elastic deflection etc....

Starting form this point of view, the aim of this project is to apply the VFC to a real car were all the mentioned parameters undergo several severe constraints. The realm of the car dynamics suggests to explicit these constraints and include them into a properly defined objective function, including the nonlinear kinematics of the suspension, their nonlinear stiffnesses, together with the modeling of the semi-active damper response.

The performance indexes analyzed in this work are divided into two categories: time domain and frequency domain, of which only the most relevant are listed here. The first category indexes are calculated for a crossing bump simulation:

- $J_{peak} = \max(|\ddot{z}_b|)$ maximum vertical body acceleration $\ddot{z}_b$ or peak reached by the vehicle;
- $J_{pitch} = \max(|\theta|)$ maximum pitch angle recorded;
- $J_{stroke} = \max(|\Delta|)$ maximum stroke, Δ reached by the front and rear suspension;
- $J_{settling} = t_{settling} : |\Delta| < \varepsilon$ time required for the suspension for dissipate the involved mechanical energy, bringing the oscillation of the suspension at below a threshold value ε.

The second indexes are calculated from the crossing simulations of random rough road:

- $J_{comf} = \sigma_{\ddot{z}_b}$ the comfort index calculated by the variance of the vertical body acceleration;
- $J_{hand} = \sigma_{\Delta_{\text{tire}}}$ the handling index or the variance of tire deflection Δ_{tire};
- $J_{fluct} = \sigma_{\theta}$ the variance of pitch angle.

The indexes calculated in the frequency domain are generally filtered between the interest frequency field. For example the comfort is usually studied between 0-20Hz and the handling is extended up to 30Hz. In the Figure 1 some couples of indexes calculated by numerical simulation are shown. In particular four different benchmark of simulation are analysed, the passive behaviour vs three different control strategies, the Skyhook, the Groundhook and the VFC [7-9]. The first two controls law are common used to compare the performances of other semi-active controls. The indexes-plane is organized in such a way to compare two J at once. Inside the plane are reported the markers representing the index value reach by the control or the passive setting. The origin of the axes represent the optimum minimum J. As regards the numerical parameters and the techniques used for tuning of the control logics reference is made to the following chapters of this paper.

In Figure 1 (left) is shown the plan relating to the minimum stroke vs. the minimum peak acceleration monitored by the car body. It is interesting to observe how the passive configuration presents a technological limit to the improvement of stroke during the passage of bump, because the J_{stroke} saturates to a default value. As regards the two classical control laws Groundhook and Skyhook are obtained reciprocal improvements J_{stroke} and for J_{peak} but are not capable of achieving combined improvements. The contrary, if you observe at the results obtained by means of the nonlinear control VFC you can get to

trade off solutions that do not represent a compromise between the two indexes but a marked improvement as worth all the proposed indicators. The same trend has also occurred with regard to the other planes as it shows.

In conclusion the VFC shows the capability to reach unexplored optimum state improving the performances of the controlled system.

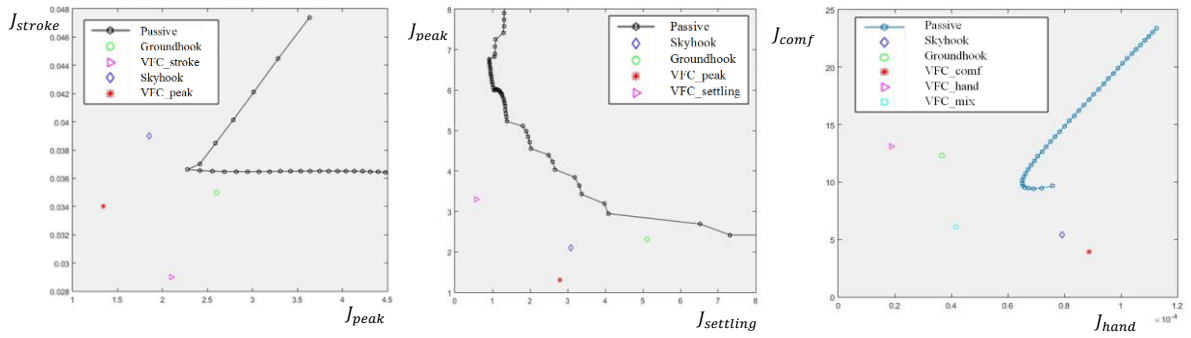

Figure 1: Indexes map: acceleration peak vs stroke (left), acceleration peak vs settling time (central), handling vs comfort (right)

2 The VFC suspension control and architecture

The experimental platform for the deployment and the VFC control tests for the control of magnetic-rheological suspensions is based on Arduino with interfaced commercial sensors. This choice is motivated by the fact of having the possibility to test different combinations of possible architectures and therefore a lot of flexibility in the combination of different sensors. The first version tested and described in this paper consists of four types of sensors, such as accelerometers, gyroscopes, magnetometers and potentiometers, connected together by a control board interconnected and connected to a central control unit *via* an ethernet network. The choice of an Ethernet-based communication configuration is motivated by the fact that the system becomes modular and can connect and disconnect the individual control units without affecting the performance of the data transmission speed. This occurs because the communication protocol is handled by suitable hardware shield, also based on an Arduino architecture. To each unit an IP address is assigned and can communicate with other control platforms in a simplified and robust way.

The architecture of the sensors is composed by four linear potentiometers mounted on the suspension, a set of eight triaxial MEMS accelerometers, a MEMS inertial platform, the IMU (Inertial Measurement Unit) with nine degrees of freedom. The latter consists of a one three-axis accelerometer, one three-axis gyroscope and one three-axis magnetometer. Four of the eight accelerometers were installed on the wheels, while the other four on the car body frame, near the joint of the suspension. The IMU is installed integral to the vehicle's body and nearby the center of gravity.

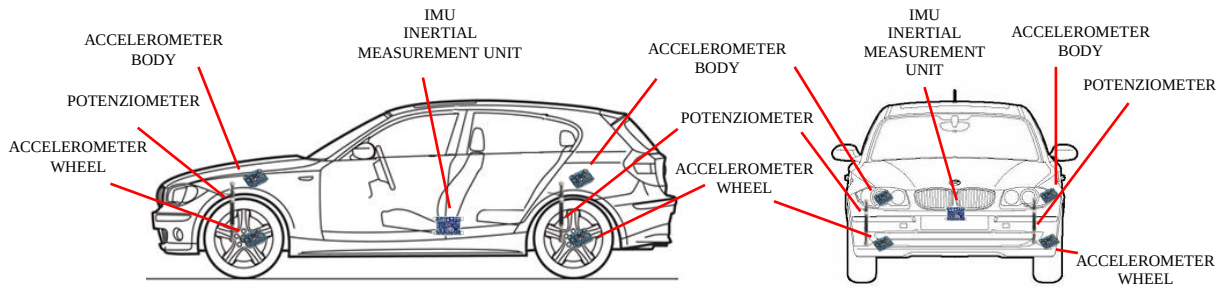

Figure 2:Sensors positions on BMW serie1

This configuration gives the opportunity to share data between the various control modules, as well as suitably combine the data with dedicated data-fusion techniques for the estimation of the optimal speed

and absolute position of the vehicle body and wheels, as well as the attitude of the vehicle. The position of the sensors is shown in Figure 2.

The control hardware consists of five platforms "Arduino Due" connected to the sensors. Four Arduino boards are positioned at the four sides of the vehicle and connected to two accelerometers, on the body and on the wheel, and to a potentiometer to measure the stroke of the suspension. The fifth Arduino board is mounted integral to the vehicle body together with the 9DOF inertial platform. The control hardware placed in proximity of the four wheels of the vehicle is the only one directly connected to the devices for the control of suspensions which will be described later in details Figure 9. The set of Arduino boards, through the Ethernet modules and the switches Figure 3, can communicate with a dedicated PC which can impart rules or strategies to adopt or can simply acquire or observe data in real-time.

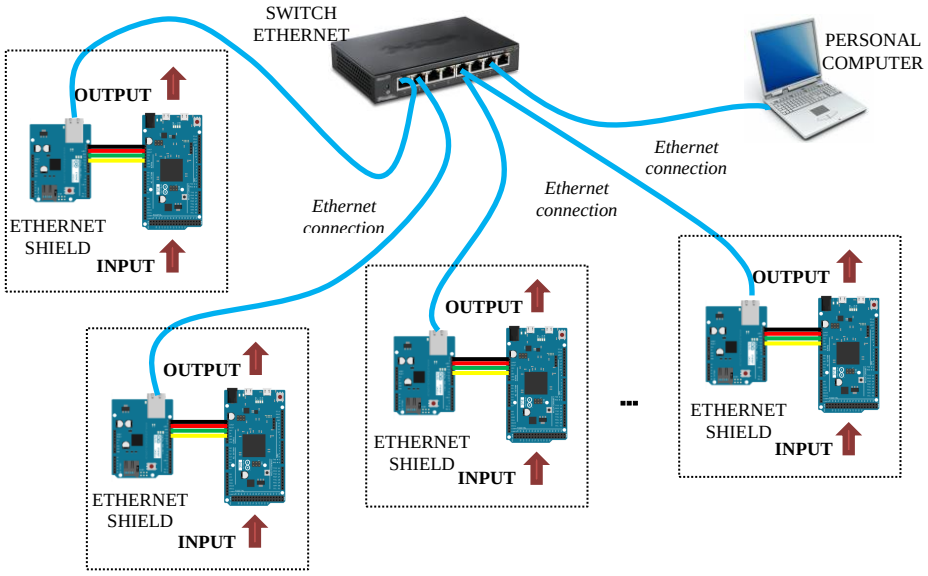

Figure 3: Arduino Ethernet configuration

3 Mathematical basis of VFC

The VFC – Variational Feedback Control is a dynamic compensator obtained through the solution of Pontryagin's minimum principle for nonlinear dynamical systems [10-15]. The novelty of the mathematical approach relies on the definition of a particular form of the objective function, as well as on certain, weak, assumptions on the form of the dynamic equation of the controlled system.

The theory of optimal control problems, can be summarized as a control algorithm that minimizes or maximizes, for a given non-linear dynamic system $\dot{\boldsymbol{x}} = \boldsymbol{f}(\boldsymbol{x}, \boldsymbol{u}, t)$, an objective function that may depend on the status of the system and the vector of inputs.

$$\begin{cases} J = \int_{t_0}^{t_f} E(\boldsymbol{x}(t), \boldsymbol{u}(t), t)dt \quad : \quad \underset{\boldsymbol{u}\in U}{Opt}\, J \\ \dot{\boldsymbol{x}}(t) = \boldsymbol{f}(\boldsymbol{x}(t), \boldsymbol{u}(t), t) \\ \boldsymbol{x}(t_0) = \boldsymbol{x}_{t_0} \end{cases} \tag{1}$$

on $\boldsymbol{u} \in U$ specifies physical restraints for the control variables $u_1(t),\ u_2(t),\ \ldots,\ u_r(t)$,

The Pontryagin solution $\boldsymbol{u}^*$ in the maximum case specifies the condition:

$$J(\boldsymbol{u}) \leq J(\boldsymbol{u}^*),\ \ \boldsymbol{u}^*, \boldsymbol{u} \in \mathrm{U} \tag{2}$$

In order to encompass the constraint condition $\dot{\boldsymbol{x}} = \boldsymbol{f}(\boldsymbol{x}, \boldsymbol{u}, t)$, the cost function can be completed by using Lagrangian multiplier $\boldsymbol{\lambda}(t) = [\lambda_1(t), \lambda_2(t), \ldots, \lambda_n(t)]^T$, leading to:

$$\begin{cases} \tilde{J} = \int_{t_0}^{t_f} E(\boldsymbol{x}, \boldsymbol{u}, t) + \boldsymbol{\lambda}^T\left(\dot{\boldsymbol{x}} - \boldsymbol{f}(\boldsymbol{x}, \boldsymbol{u}, t)\right)\, dt \;:\; Opt\,\tilde{J} \\ \boldsymbol{x}(t_0) = \boldsymbol{x}_{t_0} \end{cases} \tag{3}$$

Direct application of the variational method (or Pontryagin technique in control theory) produces the Euler-Lagrange equations in terms of $\boldsymbol{x}$,$\boldsymbol{u}$,$\boldsymbol{\lambda}$ considering initial conditions $\boldsymbol{x}_{t_0}$ and extremal conditions $\boldsymbol{\lambda}^T(t_f)$:

$$\begin{gathered} \frac{\partial E^T}{\partial \boldsymbol{x}} - \dot{\boldsymbol{\lambda}}^T - \boldsymbol{\lambda}^T \frac{\partial \boldsymbol{f}}{\partial \boldsymbol{x}} = \boldsymbol{0} \\ \frac{\partial E^T}{\partial \boldsymbol{u}} - \boldsymbol{\lambda}^T \frac{\partial \boldsymbol{f}}{\partial \boldsymbol{u}} = \boldsymbol{0} \\ \dot{\boldsymbol{x}} = \boldsymbol{f}(\boldsymbol{x}, \boldsymbol{u}, t) \\ \boldsymbol{x}(t_0) = \boldsymbol{x}_{t_0} \\ \boldsymbol{\lambda}^T(t_f)\delta\boldsymbol{x}(t_f) = \boldsymbol{0} \end{gathered} \tag{4}$$

Is possible to demonstrate that for a particular class of objective function $L(\boldsymbol{f}, \boldsymbol{y})$, where $\boldsymbol{y}$ is considered the external sources, and a non-linear dynamic system in the state $\boldsymbol{x}$, but linear in the control $\boldsymbol{u}$, then the solution of optimal control problem takes the explicit form:

$$\boldsymbol{u} = \left[\tilde{\boldsymbol{A}}\boldsymbol{S}(\boldsymbol{x}, \boldsymbol{y})\right]^{+}\left[-\tilde{\boldsymbol{A}}\boldsymbol{\varphi}(\boldsymbol{x}, \boldsymbol{y}) - \boldsymbol{B}\boldsymbol{y}\right] \tag{5}$$

where the exponent $[\quad]^{+}$ means a pseudo-inverse matrix and the other terms are:

$$\begin{gathered} L(\boldsymbol{f}, \boldsymbol{y}) = \boldsymbol{f}^T\boldsymbol{A}\boldsymbol{f} + \boldsymbol{f}^T\boldsymbol{B}\boldsymbol{y} \\ \boldsymbol{f}(\boldsymbol{x}, \boldsymbol{u}, \boldsymbol{y}) = \boldsymbol{\varphi}(\boldsymbol{x}, \boldsymbol{y}) + \boldsymbol{S}(\boldsymbol{x}, \boldsymbol{y})\boldsymbol{u} \\ \tilde{\boldsymbol{A}} = \boldsymbol{A} + \boldsymbol{A}^T \end{gathered} \tag{6}$$

The matrices $\boldsymbol{A}$ and $\boldsymbol{B}$ are the gains of the control to choose which state variable has to be minimized, $\boldsymbol{\varphi}(\boldsymbol{x}, \boldsymbol{y})$ and $\boldsymbol{S}(\boldsymbol{x}, \boldsymbol{y})$ are the non-linear component of the dynamic system $\boldsymbol{f}$ that has to be controlled. On the basis of this approach, a new class of variational controls has been identified by the authors. The applications found are applicable for semi-active and active control systems.

4 Prototyping the VFC controller

4.1 The suspension VFC controller and sensors

The simplest VFC method for suspension control is applied to a quarter of the vehicle [1]. Without going into details, the control is generated from a dynamic system of the quarter vehicle with two degrees of freedom. The damping control law, in its feedback form as a function of the state vector, is reported below, where z_b is the absolute vertical displacement of the vehicle, $z_w$is the vertical displacement of the wheel, and y is the road profile:

$$\begin{aligned} c(t) = sat_{c(t)\in[c_{min};c_{max}]} \Bigg\{ & g_0 \frac{f_{el}(z_b - z_w)}{f_{da}(\dot{z}_b - \dot{z}_w)} + g_1 \frac{f_{el_t}(z_w - y)}{f_{da}(\dot{z}_b - \dot{z}_w)} + g_2 \frac{\dot{z}_b}{f_{da}(\dot{z}_b - \dot{z}_w)} \\ & + g_3 \frac{\dot{z}_w}{f_{da}(\dot{z}_b - \dot{z}_w)} + g_4 \frac{y}{f_{da}(\dot{z}_b - \dot{z}_w)} \Bigg\} \end{aligned} \tag{7}$$

The gains g's are tuning parameters and are functions of the matrixes $\boldsymbol{A}$ and $\boldsymbol{B}$; the terms $f_{da}(\dot{z}_b - \dot{z}_w)$, $f_{el}(z_b - z_w)$ and $f_{el_t}(z_w - y)$ represent the geometric or constitutive nonlinearity of the suspension

system and the tire elasticity, damper, spring and tire stiffness characteristics, respectively; $sat_{c(t)\in[c_{min};c_{max}]}\{\}$ is the saturation function that is applied when c is no longer within the range $[c_{min}; c_{max}]$ achievable by the damping device.

At this stage, the control is ready to be used in its optimal version, if the input data from appropriate sensor are available. Unfortunately, the complete state of the system is only accessible through very specific and expensive equipment. In general, it is more reasonable to select the technologies of the on-board sensors and, where possible, estimate the state variables that are not directly measurable through data fusion techniques. For cost reasons and difficulties of commercial availability, the vehicle was equipped with accelerometers, potentiometers and IMU, as described in the above. In this case, the suspension deflection $(\mathrm{z_b} - \mathrm{z_w})$ can be directly measured by the potentiometer, while its derivatives need to be computed. Likewise, the absolute variables $\dot{z}_b, \dot{z}_w, z_b$ and z_w will be estimated with integration techniques and ad-hoc filters, e.g. a Kalman filter, applied to the data from the accelerometer and the gyroscope. More details on the data fusion techniques will be given in the following sections. The surface of the road y is accessible only through surface detection sensors, such as cameras or ultrasound systems. In this first testing phase, the surface detection sensors are not provided. In summary, the experimental apparatus shown is made of a set of sensors that read the following quantities:

$$\boldsymbol{a'}_{b_i}, \boldsymbol{a'}_{t_i}, \Delta'_i, \boldsymbol{\omega'}, \boldsymbol{h'} \tag{8}$$

where $\boldsymbol{a'} = [\ddot{x}', \ddot{y}', \ddot{z}']$ is the vector of the accelerations measured on the body frame along the three axes; the subscripts *b* and *t* stand for body and tire; primes denote the vector components in the body reference frame; while $i \in [1,2,3,4]$ denotes the four positions of the sensors, respectively: 1 for front right, 2 for front left, 3 for rear right and 4 for rear left; Δ' is the suspension stroke; $\boldsymbol{\omega'}$ and $\boldsymbol{h'}$ are the angular velocity vector measured by the gyroscope and the direction and intensity of the magnetic field, both computed in the body reference frame.

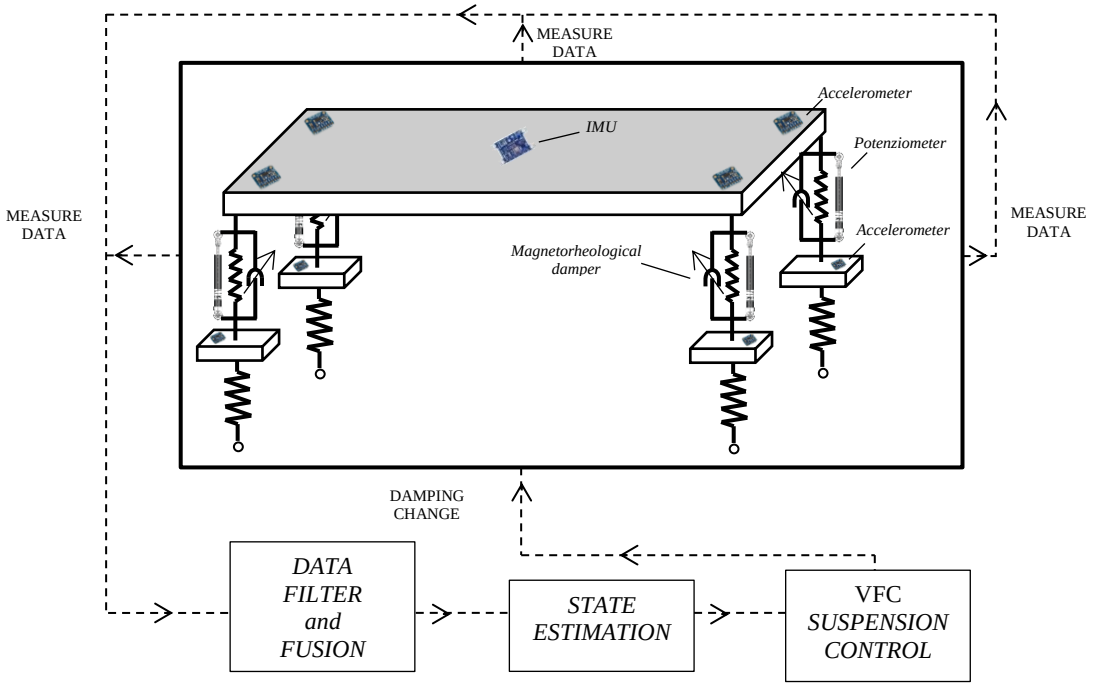

Figure 4: Sensors and control diagram for magnetic-rheological damper.

At this stage, the data from the sensors are input in the controller, which applies data filtering and fusion techniques to estimate the parameters necessary for the VFC, which will be described below (Figure 4).

4.2 The hosting vehicle

The VFC control architecture is installed on board of real car, standard production BMW Series 1 E87, part of the scientific fleet of Sapienza. This vehicle originally uses passive suspensions, therefore the first phase is devoted to the design of all the engineering modification necessary to install the magnetic-rheologic suspensions [16-19]. The *Magneride*™ [20] suspension is the magnetic-rheological (MR) damper system chosen for the project. The fundamental characteristics of the vehicle have been estimated through experimental procedures, and are reported in Table 1. They will be used later to model the whole vehicle and the tuning of the VFC control logic through a simulation. The measure of the centre of gravity position and the elastic stiffness of the suspension is made by load cells and linear potentiometers installed on the suspensions. The stiffness is almost constant when varying the suspension stroke, while the procedure for the damping estimation is explained in the following sections.

MAIN CHARACTERISTICS OF VEHICLE	VALUES
Vehicle weight *(Measured with passengers)*	1,530 kg
Front tire mass *(estimated)*	35 kg
Rear tire mass *(estimated)*	35 kg
Front stiffness (*Measured*)	22,600 N/m
Rear stiffness *(Measured)*	46,800 N/m
Distance between front wheel and center of gravity *(Measured)*	1.3 m
Distance between rear wheel and center of gravity *(Measured)*	1.4 m

Table 1: Main characteristics of vehicle

The vehicle mounts a multi-link Mac Pherson system as the front suspension, a sophisticated structure where the usual triangular bottom link is replaced with two transverse links with spherical joints. These links connect the wheel-carrier to the frame.

Figure 5: CAD of the original BMW front kinematic suspension at (left) and the rear one at (right).

The rear suspension is a five link system with spherical joints. First, the suspension was reverse engineered and a CAD model Figure 5 and the kinematic solution were produced. The kinematic solution is fundamental to identify the transfer function between the difference of the vertical displacement of wheel and body and the stroke of the suspension, and to correlate the potentiometer output with the stroke of the suspension.

4.3 The magnetic-rheological damper

The dampers chosen to implement the VFC are the *Magneride*, produced by BWI [20], which were adapted into the BMW suspension system. Several changes were deemed necessary, following careful kinematics, dynamics and especially structural analyses.

MagneRide has no mechanical valves or small moving parts (Figure 6). The shock absorber is a monotube damper with a floating piston De Carbon scheme like. *MagneRide* uses a Magneto-Rheological (MR) damper fluid which contains tiny metallic particles that can be quickly but temporarily magnetized by flowing a current through the electrical coils in the damper piston. When the current is off, the particles are randomly dispersed and the damper is in its softest setting. Applying a current, magnetizes the particles which in turn attract each other in proportion to the strength of the magnetic field, increasing the resistance to flow and stiffening the damping. The result is the ability to vary the damping force almost instantaneously over a wide range, just by varying the applied current. The system has low energy requirements, typically less than 20W absorbed by each damper. *MagneRide* was first used by General Motors in the Cadillac Seville STS (2002) and is now used as a standard suspension or an option in many models for Cadillac, Buick, Chevrolet, and other GM vehicles. It can also be found on some non-US vehicles such as Holden Special Vehicles, Ferrari, and Audi.

In our prototype *MagneRide* is controlled by an amplifier managed by the Arduino board. The chosen amplifier is produced by LORD [21], and it is able to change the current flowing through the shock absorbers in such a way that the damping is varied in real time. The amplifier consists of: (i) a power supply input at 12VDC; (ii) output connectors through which the current is sent to the damper; (iii) a BNC terminal to input a PWM control signal at about 1kHz, managed by the Arduino board (Figure 9).

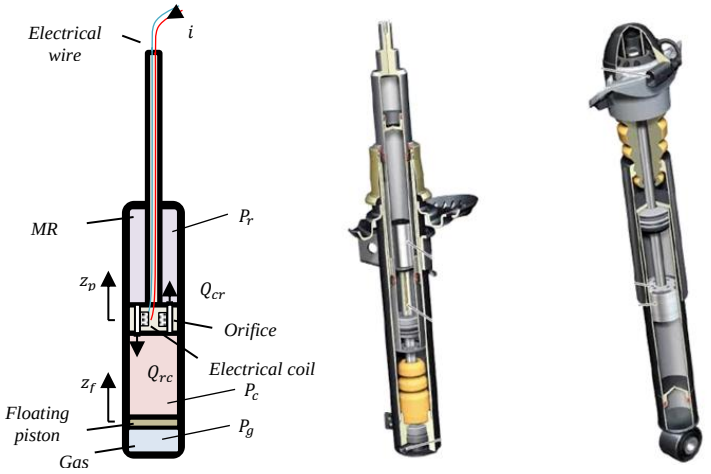

Figure 6: The magnetorheological damper installed on BMW (*Magneride* of BWI Group)

In the forward damper, it was necessary to modify the inner diameter of the BMW wheel-carrier, change the lodging of the spring in order to have the same static deflection and therefore to operate in the same condition as the original suspension. Moreover, the upper dome had to be entirely redesigned (Figure 7). Regarding the rear *MagneRide*, the lower end was modified by replacing the pre-existing hinge with a spherical joint for the multi-link kinematics.

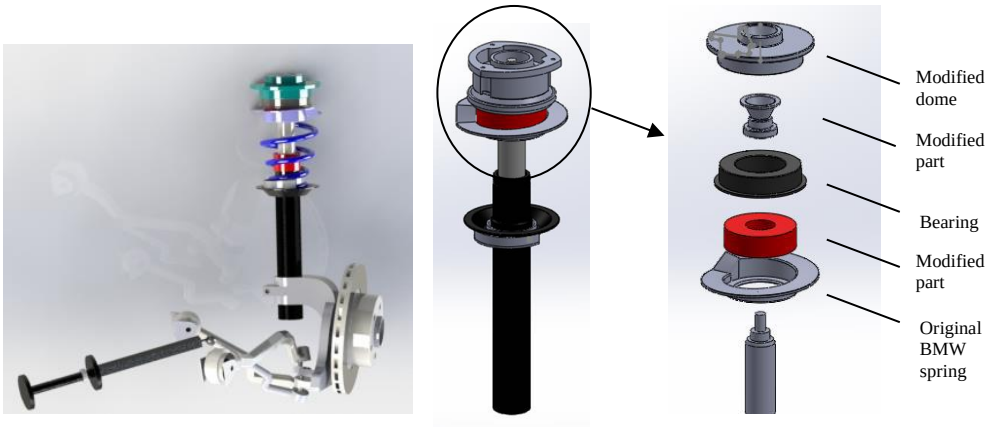

Figure 7: CAD of the front *Magneride* suspension and changing the upper dome.

4.4 Controller hardware and sensors

In this section, the main characteristics of the set of sensor used on board of the vehicle are illustrated (see Figure (10)):

1-Potenziometer sensor: The MLS-0952 (Motorsport Linear Sensor) is a linear, low noise potentiometer, the maximum speed attainable by the potentiometer is about 10 m/s. The potentiometer is connected to the 5 VDC power supply pin, which is the value of the full scale. The analogue output is instead redirected to an analogue pin of the controller.

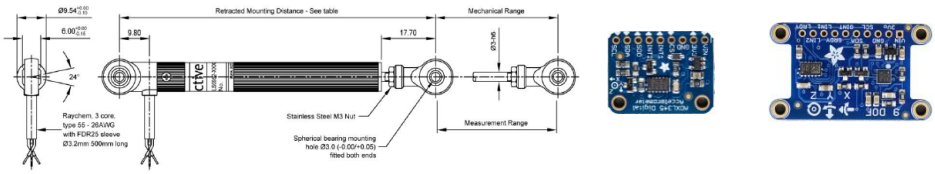

Figure 8: Potenziometer *Motorsport Linear Sensor* (left), Accelerometer and IMU (central and right).

Car body and tire accelerometer sensors: The ADXL345 is low power 3-axis MEMS accelerometer with high resolution (13-bit) measurement at up to +-16 g. Digital output data is I2C digital interface. Its high resolution (4 mg/LSB) enables measurement of inclination changes less than 1.0 degrees;.

Inertial Measurement Unit sensor: The inertial-measurement-unit chosen is Adafruit 9-DOF that combines three sensors: 3 axes of accelerometer data, 3 axes gyroscopic, 3 axes magnetic (compass). The L3DG20H is the gyroscope hardware and LSM303DLHC is the accelerometer and compass hardware. All of them use I2C and is possible to communicate with all of them using only two wires with a resolutions up to 13-bit. The L3GD20H 3-axis gyroscope is a type of sensor that can sense twisting and turning motions up to ±2000 degree-per-second scale. Inside the LSM303DLHC there are two sensors, one is a classic 3-axis accelerometer, the other is a magnetometer that can sense where the strongest magnetic force is coming from used to detect magnetic north. LSM303DLHC has linear acceleration full-scales up to ±16g and a magnetic field full-scale up to ±8.1 gauss.

Controllers: In Figure 9, the connection diagrams of the Arduino controllers with the sensors are reported. In particular, the reference platform used is Arduino Due, a board that operates in 32-bit to achieve the maximum performance. Overall, five Arduino boards are installed, four of which being next to every wheel to read the accelerometers on the body and wheel and the potentiometer and to control the current amplifier to change the damping characteristics of the MR. The central Arduino board is connected to the 9 DOF IMU, and its purpose is to compute the attitude of the vehicle through filtering and data fusion algorithms. In Figure 9, it is possible to see the analog connection with the potentiometer with a resolution of a tenth of a millimeter; an I2C link with the two ADXL345 accelerometers, which allows long wiring and communication stability through suitably sized pull-up resistors; a PWM connection for the control of

the current sent to the MR damper. In Figure 9, the link with the 9 DOF IMU platform is also I2C. As described above, all the boards have a specific shield to communicate with one another and a dedicated PC through the ethernet UDP protocol.

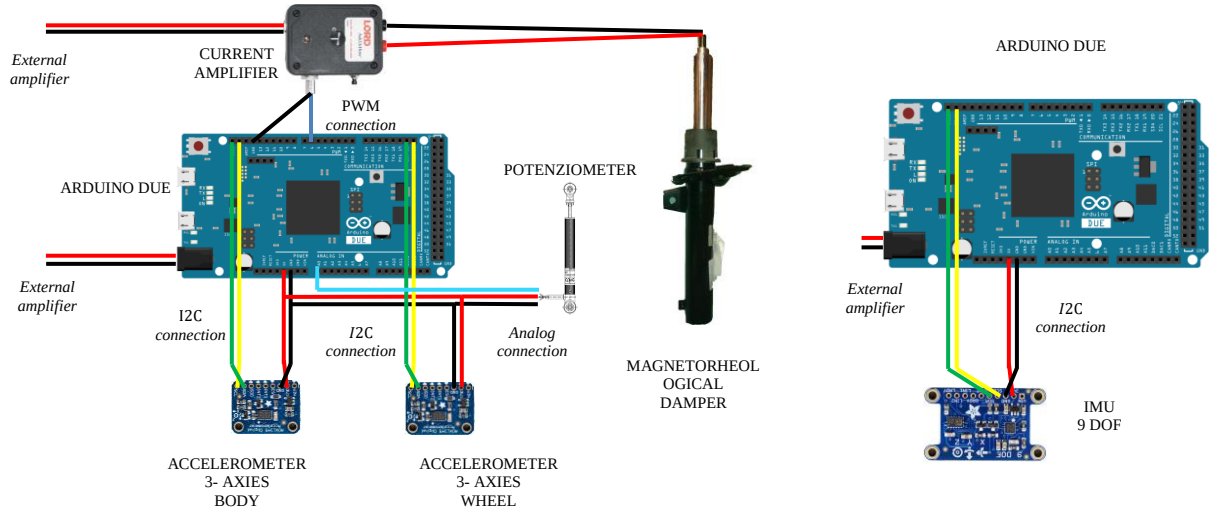

Figure 9: Arduino layout: a quarter wire connection diagram (left), the central Arduino with IMU (right)

4.5 Data fusion and filtering

Sensor fusion algorithms consist of technical specifications developed in order to organize and manage data from different types of sensors, with the purpose of obtaining information about the system state which is not directly observable or of improving the observability of quantities which can be partly measured by the available sensors. The data fusion method used here involves combining the data from the IMU inertial platform in order to correctly compute the attitude of the vehicle and its angular velocities, and to obtain the absolute position and vertical velocity starting from the measure of the accelerometer. One of the simplest filters for the IMU sensors is the complementary filter. In the Figure 10 a complete diagram of the data filtering and operation is shown to prepare the VFC input data. This filter gives a direct estimation of the pitch and roll of the body using six degrees of freedom of the IMU platform (three accelerometer, three gyroscope). The filter is made of a linear combination of the attitude angles calculated by means of the accelerometer and gyroscope. This combination is made to improve the estimation of pitch and roll in order to mitigate both the inherent errors of the sensors due to the limits of measure range, linearity of response, frequency range, etc., and those relating to the data measure itself, because of noise. Right after the correct estimations of the pitch, roll and yaw are used to rotate the accelerometer data measured in the body reference frame, and they are converted to the fixed reference frame. In this way, the vertical component of the acceleration can be extracted, and it is possible to cancel out the gravitational acceleration, which is constantly measured by the MEMS sensors. Gravity needs to be eliminated because it would cause a drift error during the process of integration of the vertical accelerations. Last, the orientation of the body, together with the data from the potentiometer and the kinematic laws of the suspensions, allows to calculate the attitude of the accelerometers of the wheels and to obtain their absolute vertical accelerations, necessary to implement the VFC control.

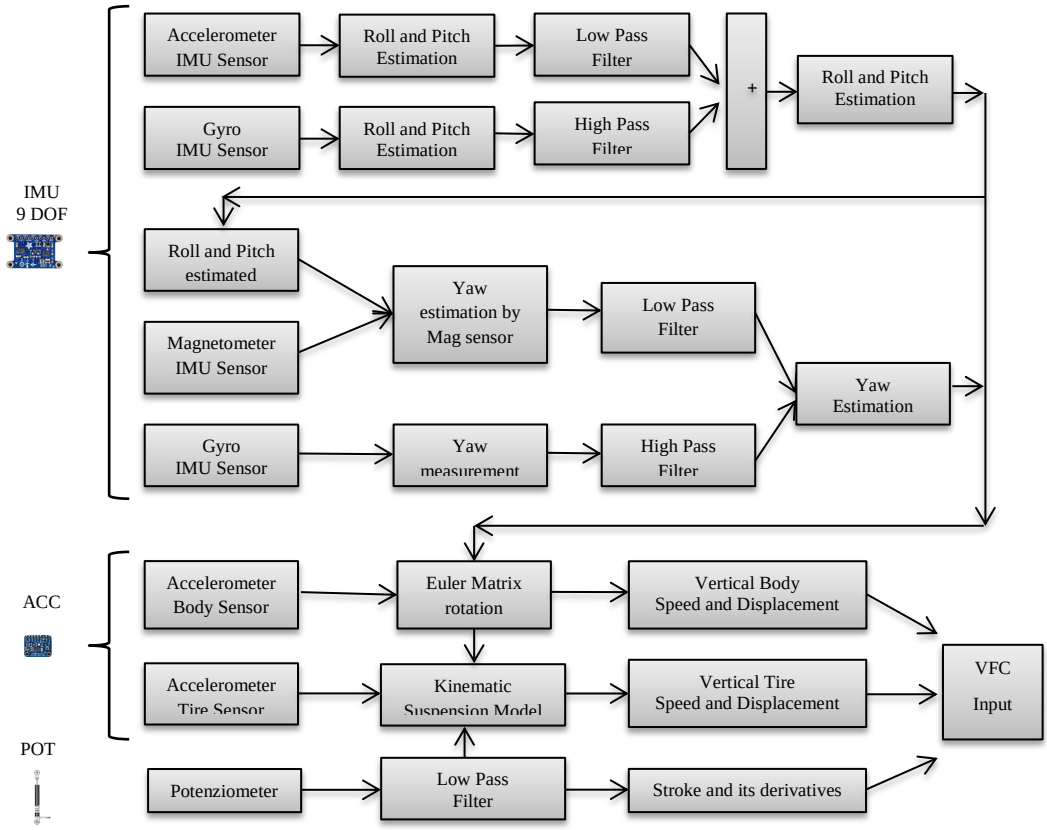

Figure 10: Data fusion and filtering diagram for VFC data input.

5 VFC tuning

The VFC control law is directly implemented on the four Arduino boards managing the four suspensions. Analysing the control equation, it is possible to see that the gains are not determined *a-priori* but, as in most control logics, they play the role of tuning parameters. Since the VFC is intended for nonlinear systems, it is not possible to define *a-priori* a direct relation between the gains and the system response. In fact the VFC, through the specific form of its functional, is able to generate a control that can in general minimize the objective function depending on the system state vector, but this last can be only accessed indirectly, through the characteristics found by the VFC controller. As a result, there is no direct correlation between handling/comfort and the gains of the control, which is the reason why a tuning procedure to regulate the feedback control is needed.

For the tuning of the gains, the first step is the modeling of the vehicle system to test numerically the control logic, and then a method of identification of the gains by means of Genetic Algorithms GA is applied. In the field of artificial intelligence, a GA is a search heuristic that mimics the process of natural selection. Genetic algorithms generate solutions to optimization problems using techniques inspired by natural evolution, such as inheritance, mutation, selection and crossover. In particular, the method applied to identify the best gains minimizes an objective function. The objective functions are the optimum indicators reported at the beginning of the paper. So if we want to find, for example, the best gains for maximum comfort, our control evaluation function will look like:

$$J_{comf} = \sigma_{\ddot{z}_b} \tag{9}$$

At this stage, the genetic algorithm randomly generates an initial set of gains and executes the simulation of the VFC-controlled model. At the end of the simulation, the time history of the acceleration is known, and it is possible to evaluate the variance and therefore the J_{comf}. Then, the genetic algorithm reassigns new sets of gains to the VFC according to how much the J_{comf}improves or worsens, with specific

techniques of the algorithm. The synthetic diagram of the operation of the tuning procedure is shown in Figure 12. GAs belong to the family of advanced Montecarlo methods, for which convergence or the reaching of the absolute minimum are not guaranteed. Nonetheless, they are excellent methods where no direct correlation exists between the quantities and where a strong nonlinearity is present. The results obtained with the GA are reported in the Figure 12. The results of the tuning procedure are derived from a dynamic half-car model, in which the stroke-end of the suspension is also modelled. This is a fundamental property of the system, which is necessary to take into account to achieve optimal results in practical applications. The equation used for the analysis are:

$$\begin{cases} \ddot{z}_b = \frac{1}{m_b}\left[-k_f\left(z_b + l_f\theta - z_{wf}\right) - k_r(z_b - l_r\theta - z_{wr}) - F_{D_f} - F_{D_r}\right] \\ \ddot{\theta} = \frac{1}{J}\left[-l_f k_f\left(z_b + l_f\theta - z_{wf}\right) + l_r k_r(z_b - l_r\theta - z_{wr}) - l_f F_{D_f} + l_r F_{D_r}\right] \\ \ddot{z}_{wf} = \frac{1}{m_{wf}}\left[-k_{tf}\left(z_{wf} - y_f\right) - k_f\left(z_{wf} - z_b - l_f\theta\right) - F_{D_f}\right] \\ \ddot{z}_{wr} = \frac{1}{m_{wr}}\left[-k_{tr}(z_{wr} - y_r) - k_r(z_{wr} - z_b - l_r\theta) - F_{D_r}\right] \\ \boldsymbol{\Psi}\left(z_b, \theta, z_{wf}, z_{wr}\right) = \mathbf{0} \end{cases} \tag{10}$$

where the subscripts $b, wf, wr, tf, tr, t, f, r$ are designate: body, front wheel, rear wheel, front tire, rear tire, tire, front and rear, respectively; where the coordinate $z, \dot{z}, \ddot{z}$ are the displacement and its derivative of the three m sprung and unsprung mass; θ is the pitch coordinate and J is the momentum of inertia; l is the distance between the centrum gravity and the suspension link; y is the external sources; k is the stiffness elastic element. The F_{D_f} and F_{D_r} are the controlled damping forces and $\boldsymbol{\Psi}$ are algebraic constraints representing the end stroke.

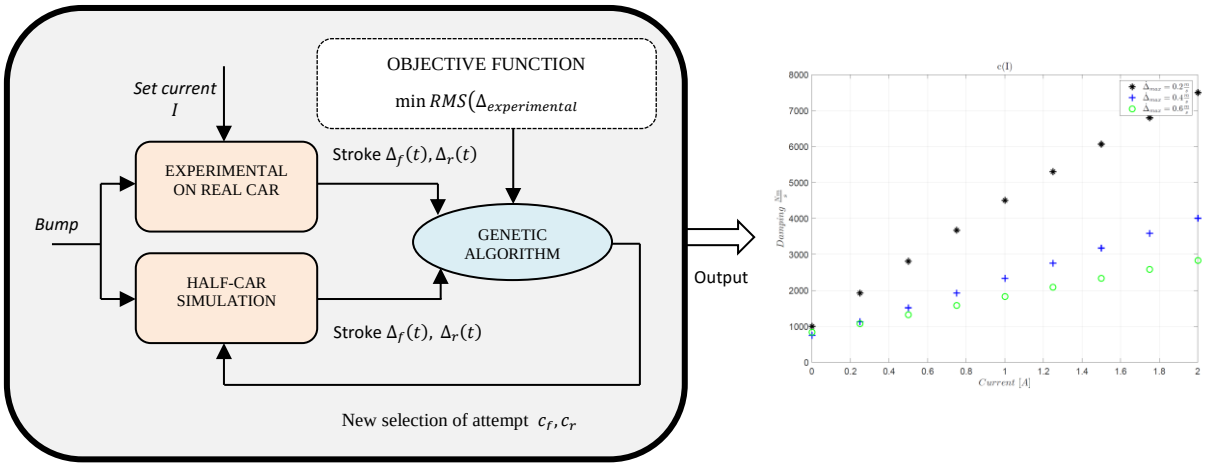

Figure 11: Genetic Algorithm apply to the identification of the map I(c), current vs damping

To develop such a tuning procedure it has been necessary to model accurately the entire system, identifying the fundamental characteristics of the dampers and the associated current. Two major problems were encountered to develop the tuning procedure. The first is the identification of the function that associates the damping suggested by VFC method and the current to be actually injected into the damper. The second is the simulation of the dynamic behaviour of the real response of the damper inside the vehicle. This requires a careful and effective modeling, otherwise it would generate results that do not overlap with the experiments. Regarding the first identification of the map $I(c)$, where I is the current and c is the damping, ad-hoc experiments were carried out. In particular, a series of tests have been developed where the response over a bump at a constant speed with different current levels was analysed. The current was varied in discrete form according to the following values of measured current in amperes: $I = [0; 0.25; 0.5; 0.75; 1; 1.25; 1.5; 1.75; 2]$. At this point, the potentiometric experimental data, relative to the stroke, are compared with the stroke simulated by the half-car model in which the only parameter to be changed is the front and rear damping. The simulations are carried out in such a way as to comply with

the crossing speed condition and the profile of the bump, and a first guess value, both for the front and the rear damping, is initially imposed. Subsequently, an iterative algorithm was developed, always based on GA, for the detection of that optimal c of the front and rear, such that good results are obtained with regard to the difference of the two stroke curves, experimental and numerical (Figure 11).

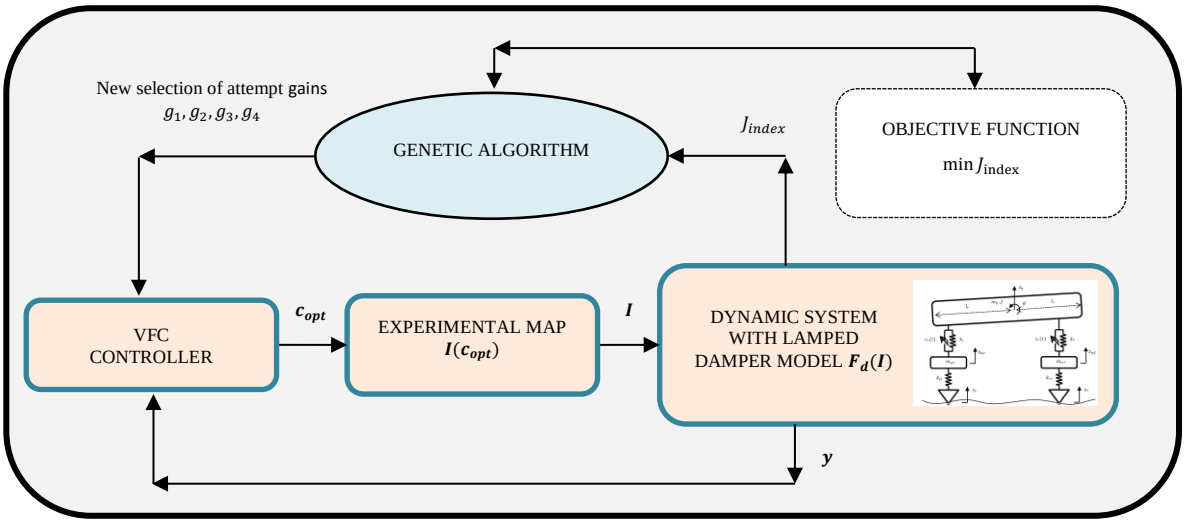

Figure 12: Genetic Algorithm apply to the gains VFC identification

Regarding the second identification, that is the simulation of an MR damper that can behave similarly to the experiments, a lumped model has been developed. In summary, the following set of equations is used:

$$\begin{aligned} &\boldsymbol{M}\ddot{\boldsymbol{x}} = \sum \boldsymbol{F}\left(\boldsymbol{x}, \dot{\boldsymbol{x}}, I, P_c, P_r, P_g\right) \\ &\left.\begin{aligned} &\dot{P}_c = -\frac{\beta}{V_c(\boldsymbol{x})}\left(Q + \dot{V}_c(\dot{\boldsymbol{x}})\right) \\ &\dot{P}_r = -\frac{\beta}{V_r(\boldsymbol{x})}\left(Q + \dot{V}_r(\dot{\boldsymbol{x}})\right) \\ &P_g V_g^{\gamma} = P_{g0} {V_{g0}}^{\gamma} \\ &Q = f(\dot{\boldsymbol{x}}, I, P_c, P_r, P_g) \end{aligned}\right\} \text{for rear and front damper} \\ &\boldsymbol{\Psi}(\boldsymbol{x}) = \boldsymbol{0} \end{aligned} \tag{11}$$

With $\boldsymbol{x} = \left[z_b, \theta, z_{wf}, z_{wr}, z_f\right]^T$ the state vector of the masses, P_c, P_r and P_g the pressures of the compression chamber, the rebound chamber and gas chamber, Q is the rate flow in function of $\dot{\boldsymbol{x}}$, the current I and the $\boldsymbol{\Psi}(\boldsymbol{x})$ are algebraic function which identify the constraint like the end stroke of each mass. At this point an iterative optimal VFC gains identification procedures is done by the GA and the result are directly test on board to confirm the goodness results.

6 Results and conclusions

The experimental results above show how the selected gains in the VFC strategy have an influence on the performance of the control. The conducted experimental activities show excellent results for the VFC control *vs* passive configuration. The tests program included random paths consisting of manoeuvres involving several different kinds of road-input as a bump, bents, braking, accelerations, random paths on fast roads etc. Figure 13 shows the Power Spectra Density - PSD with ordinate logarithmic scale. In Figure 13-1 the vertical acceleration of the car body is shown, and in Figure 16-2 the vertical acceleration zoom on at low frequencies is shown. In this particular case the tuning of VFC produces a compromise between simultaneous improvement of comfort, stroke and handling. In Figure 13-3 the acceleration of the wheel is shown rather than the direct tire deflection measurement that requires expensive and complicated devices. In fact, often a negative consequence of some controls is the chattering phenomenon or high

frequency oscillations affecting the control dynamics that amount to mechanical equipment vibrations and to the wheel hop response. The absence of such phenomenon is also observed from the Figure 13-4, that shows the PSD of the stroke with a trend similar to the passive device, except in the frequency range 15-30Hz.

These reported results show how the VFC is able to control most aspects of the vehicle dynamic response with uncompromising and proving to be a robust controller able to make improvements on many fronts.

The experimental campaign is organized in such a way as to define a procedure robust and optimized tuning. The tests are performed to calculate the optimal index as shown at the beginning of the paper for different paths and different bump cross.

Future developments and future investigations will be devoted to a detailed analysis of additional specific manoeuvres such as rapid and slow steering, change lane, single-bump, brake accelerated, smooth road and rough road. Finally the applications to high-speed marine vehicles will be explored in the frame of the Sapienza project SEALAB where fluttering of skids problems heavily affect the navigation [23,24].

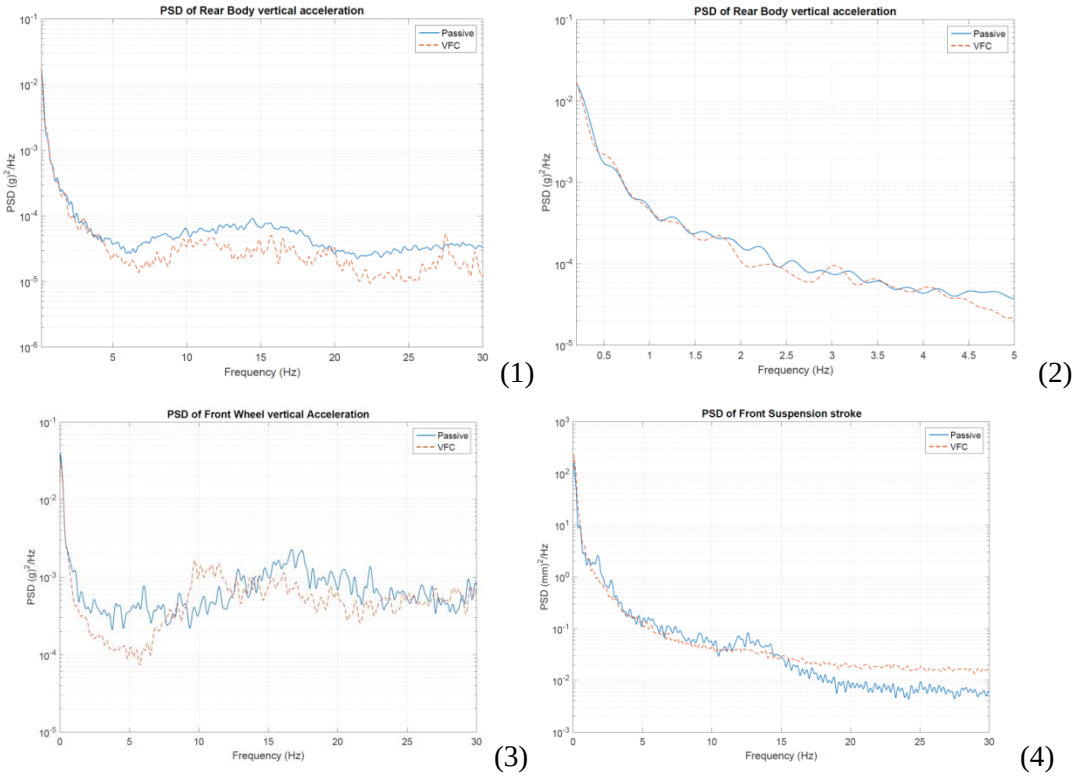

Figure 13: PSD of experimental activities, passive vs VFC: (1) and (2) show the vertical acceleration of the body, (3) and (4) show the wheel acceleration and stroke PSD.

References

[1] G. Pepe, A. Carcaterra, *VFC – Variational Feedback Controller and its application to semi-active suspensions*, Mechanical Systems and Signal Processing, (2016).

[2] G. Pepe, A. Carcaterra, *VFC - Variational Feedback Control applied to semi-active car suspensions, in NOVEM2015*, (2015).

[3] G. Pepe, I. Giorgio, A. Carcaterra, D. Del Vescovo, A. Sestieri, *Semiactive vibration control via VFC-Variational Feedback by piezoelectric actuation, NOVEM2015,* (2015).

[4] G. Pepe, A. Carcaterra, I. Giorgio, D. Del Vescovo, *Variational Feedback Control for a nonlinear beam under an earthquake excitation*, Mathematics and Mechanics of Solids, (2014).

[5] G. Pepe, A. Carcaterra, *Semi-Active Damping by Variational Control Algorithms, presented at the Proceedings of the 9th International on Structural Dynamics, EURODYN 2014, Porto, Portugal, 30 June - 2 July,* (2014).

[6] G. Pepe, A. Carcaterra, *A new semi-active variational based damping control, MESA 2014 - 10th IEEE/ASME International Conference on Mechatronic and Embedded Systems and Applications, Conference Proceedings,* (2014).

[7] S. Savaresi, C. Poussot-Vassal, C. Spelta, O. Sename, L. Dugard, *Semi-Active Suspension Control Design for Vehicles*, Elsevier, (2010).

[8] S. M. Savaresi, C. Spelta, *Mixed sky-hook and ADD: Approaching the filtering limits of a semi-active suspension*, Journal of Dynamic Systems, Measurement and Control, Transactions of the ASME, vol. 129, (2007), pp. 382-392.

[9] D. Karnopp, Crosby, M., Haewood, R., *Vibration control using semi-active force generators*, Journal of Engeneering for Industry, vol. 2, (1974), pp. 619-626.

[10] P. Loreti, G. V. Caffarelli, *Variational solutions of coupled Hamilton-Jacobi equations,* Applied Mathematics and Optimization, vol. 41, (2000) , pp. 9-24.

[11] V. Komornik, P. Loreti, E. Zuazua, *On the Control of Coupled Linear Systems*, Control and Estimation of Distributed Parameter Systems. vol. 126, W. Desch, F. Kappel, and K. Kunisch, Eds., ed: Birkhäuser Basel, (1998), pp. 183-189.

[12] D. E. Kirk, *Optimal Control Theory: An Introduction*: Dover Publications, (2012).

[13] A. E. Bryson, *Applied Optimal Control: Optimization, Estimation and Control*: Taylor & Francis, (1975).

[14] A. A. Agrachev, P. Nistri, G. Stefani, *Nonlinear and Optimal Control Theory: Lectures Given at the C.I.M.E. Summer School Held in Cetraro*, Italy, June 19-29, 2004: Springer, (2008).

[15] D. Liberzon, *Calculus of Variations and Optimal Control Theory: A Concise Introduction*, Princeton University Press, (2011).

[16] D. Q. Truong, K. K. Ahn, *Identification and application of black-box model for a self-sensing damping system using a magneto-rheological fluid damper*, Sensors and Actuators A: Physical, pp. 305-321, (2010).

[17] M. R. Jolly, J. W. Bender, J. D. Carlson, *Properties and Applications of Commercial Magnetorheological Fluids*, Journal of Intelligent Material Systems and Structures, vol. 10, pp. 5-13, (1999).

[18] A. Milecki, M. Hauke, *Application of magnetorheological fluid in industrial shock absorbers*, Mechanical Systems and Signal Processing, vol. 28, pp. 528-541, (2012).

[19] H. Metered, P. Bonello, S. O. Oyadiji, *The experimental identification of magnetorheological dampers and evaluation of their controllers*, Mechanical Systems and Signal Processing, vol. 24, pp. 976-994, (2010).

[20] BWI Group *http://www.bwigroup.com/en/*

[21] Lord. (2008). *Technical report, Lord*. Available: http://www.lord.com

[22] N Roveri, A Carcaterra, A Akay, *Vibration absorption using non-dissipative complex attachments with impacts and parametric stiffness*, The Journal of the Acoustical Society of America 126 (5), 2306-2314, (2009)

[23] A Carcaterra, D Dessi, F Mastroddi, *Hydrofoil vibration induced by a random flow: a stochastic perturbation approach*, Journal of Sound and Vibration 283 (1), 401-432, (2009)

[24] A Carcaterra, A Scorrano, G Pepe, *SEALAB: Aero-hydro mechanics of a three-wings jumping vehicle*, HSMV, (2011)